Pure Appl. Geophys. 173 (2016), 1783–1801

DOI 10.1007/s00024-015-1206-7

Pure and Applied Geophysics

Performance of WRF-ARW model in real-time prediction of Bay of Bengal cyclone 'Phailin'

M. Mandal,[1] K. S. Singh,[1] M. Balaji,[1] and M. Mohapatra[2]

Abstract—This study examines the performance of the Advanced Research core of Weather Research and Forecasting (ARW-WRF) model in prediction of the Bay of Bengal cyclone 'Phailin'. The two-way interactive double-nested model at 27 and 9-km resolutions customized at Indian Institute of Technology Kharagpur (IITKGP) is used to predict the storm on real-time basis and five predictions are made with five different initial conditions. The initial and boundary conditions for the model are derived from the Global Forecasting System (GFS) analysis and forecast respectively. The track of storm is well predicted in all the five forecasts. In particular, the forecast with less initial positional error led to more accurate track and landfall prediction. It is observed that the predicted peak intensity and translation speed of the storm depends strongly on initial intensity error, vertical wind shear and vertical distribution of maximum potential vorticity. The trend of intensification and dissipation of the storm is well predicted by the model in terms of central sea level pressure (CSLP). The intensity in terms of maximum surface wind (MSW) is under-predicted by the model and it is suggested that the MSW estimated from predicted pressure drop may be used as prediction guideline. The storm intensified rapidly during its passage over the high Tropical Cyclone Heat Potential zone and is reasonably well predicted by the model. Though the magnitude of the precipitation is not well predicted, distribution of precipitation is fairly well predicted by the model. The track and intensity of the storm predicted by the customized WRF-ARW is better than that of other NWP models. The landfall (time and position) is also better predicted by the model compared to other NWP models if initialized at cyclonic storm stage. The results indicate that the customized model have good potential for real-time prediction of Bay of Bengal cyclones and encourage further investigation with larger number of cyclones.

Key words: Prediction, tropical cyclone, WRF model, intensity, track, Phailin.

1. Introduction

Landfalling tropical cyclones (TCs) are one of most feared and deadly meteorological phenomena in the coastal regions worldwide. The devastation is mainly due to the strong wind, heavy rainfall and associated storm surges (Emanuel 2005). Besides human causality TCs cause huge damage to property. The loss of life and property due to these landfalling TCs can be significantly reduced by providing more accurate prediction of track, landfall (location and time) and intensity of the storm. So, it is very important to predict the TCs as accurately as possible. There has been significant improvement in numerical prediction of TCs in last three decades. This is mainly due to improvement in high-resolution dynamical models, understanding of physical processes and data assimilation technique for providing better initial condition to the models. However, the track and intensity prediction of the TC remain a challenging task for atmospheric scientist and operational forecasters.

In last two decades, the focus is on high-resolution mesoscale prediction. Pattanayak and Mohanty (2008) evaluated the performance of the Advanced Research core of Weather Research and Forecasting (WRF-ARW), WRF-NMM and MM5 model for the prediction of very severe cyclonic storm (VSCS) Sidr. It indicates that WRF-ARW model has better forecast skill in terms of intensity prediction, but WRF-NMM has better skill in predicting the track. Davis *et al.* (2008) studied the performance of the WRF-ARW model towards real-time prediction of five land-falling Atlantic hurricanes during 2005. They found that the performance of WRF-ARW model is occasionally superior to other operational forecasts. Several studies are conducted to investigate sensitivity of various physical processes (Mandal

[1] Centre for Oceans, Rivers, Atmosphere and Land Sciences, Indian Institute of Technology Kharagpur, Kharagpur 721 302, India. E-mail: mmandal@coral.iitkgp.ernet.in

[2] Cyclone Warning Division, IMD, Mausam Bhavan, Lodi Road, New Delhi 110 003, India.

et al. 2004; Pattanayak *et al*. 2012; Deshpande *et al*. 2010, 2012; Osuri *et al*. 2011; Srinivas *et al*. 2007, 2012; Bhashkar Rao and Prasad 2006), model resolution (Mandal *et al*. 2003; Bhaskar Rao *et al*. 2010) and impact of initial and boundary conditions (Mandal and Mohanty 2006; Sandeep *et al*. 2006; Abhilash *et al*. 2007; Govindankutty *et al*. 2010; Singh *et al*. 2008, 2011; Rakesh *et al*. 2009; Rakesh and Goswami 2011; Mohanty *et al*. 2010; Kumar *et al*. 2011; Osuri *et al*. 2012; Srinivas *et al*. 2010, 2013) towards mesoscale simulation of the Bay of Bengal cyclones. Some studies on numerical simulation of TC and monsoon depression over North Indian seas are also reported (Roy Bhowmik 2003; Kumar *et al*. 2010; Routray *et al*. 2010; Raju *et al*. 2011). India Meteorological Department (IMD) is presently using three regional models, Quasi-Lagrangian Model (QLM), WRF, and Hurricane WRF (HWRF) for short range prediction and Global model T574L64 for medium range forecast (7 days) of TCs in North Indian seas. IMD is also using a multi-model ensemble (MME) forecast to generate real-time prediction of TC track with IMD-GFS, IMD-WRF, GFS-NCEP, UKMO and JMA models as member (Kotal and Roy Bhowmik 2011). Tyagi *et al*. (2010) reported that the mean track forecast errors in real-time prediction using QLM are about 92, 152, 235 and 375 km in 12, 24, 48 and 72 h forecasts, respectively. The operational track forecast errors of IMD are 140, 262 and 386 km in 24, 48 and 72 h forecasts, respectively (Mohapatra *et al*. 2013a). Similarly the operational intensity forecast errors are 11, 14 and 20 knots in 24, 48 and 72 h forecasts (Mohapatra *et al*. 2013b). Comparing with other Ocean basins, the operational forecast errors of IMD are still significantly higher than that of National Hurricane Centre, USA for TCs over North Atlantic Ocean (Mohapatra *et al*. 2013a, b). Hence, there is further scope for improvement in track and intensity forecasts based on numerical weather prediction models, especially customized regional/mesoscale models.

Recently, a very severe cyclonic storm, PHAILIN crossed east coast of India near Gopalpur (Odisha) around 1700 UTC of 12th October 2013 with a sustained maximum surface wind speed of 215 kmph.

In this study, a customized version of ARW-WRF model is used for real-time prediction of the VSCS 'Phailin'. The objective is to investigate the capability of the modeling system in predicting the track, intensity and landfall of the storm and some of its specific features. A brief description of the storm 'Phailin' and associated synoptic features are presented in Sect. 2. The configuration of WRF model used in the present study is described in Sect. 3. The numerical experiments conducted and data used are discussed in Sect. 4. The initial conditions used for the simulations are investigated in Sect. 5. The results obtained and related discussions are presented in Sect. 6 followed by summary in Sect. 7.

2. *A brief description of VSCS Phailin*

The VSCS Phailin initially appeared as a well-marked low pressure area over North Andaman Sea on 7th October 2013 (IMD 2013) and concentrated into a depression at 00:00 UTC of 8th October centered near (12.0°N, 96.0°E). It moved northwestward and intensified into a deep depression in the morning of 9th October. Moving in west–northwestward direction, it crossed Andaman Islands near Mayabandar at 09:00 UTC of 9th October. The system moved slowly over east central Bay of Bengal and intensified into a cyclonic storm named 'Phailin' around 12:00 UTC. Moving westward, the storm intensified into a severe cyclonic storm (SCS) at 03:00 UTC and further into a VSCS over east central Bay of Bengal around 06:00 UTC of 10th October. The storm intensified further and attained its maximum intensity around 03:00 UTC of 11 October. At this stage, it was located near (16.0°N, 88.5°E) with wind speed 115 knots and central sea level pressure (CSLP) 940 hPa. Moving in northwestward direction the storm crossed east coast of Indian near Gopalpur, Odisha, around 17:00 UTC of 12 October 2013. After the landfall, the system moved north–northwestward for some time and then northward and finally north–northeastward up to southwestern part of Bihar. The storm weakened gradually into an SCS by 03:00 UTC of 13 October and into cyclonic storm around 06:00 UTC. It further weakened into a deep depression over north Chhattisgarh and adjoining Odisha and Jharkhand by 12:00 UTC of 13 October and into a depression around 03:00 UTC of 14 October over

southwest Bihar. The observed track of the storm is shown in Fig. 1. The salient features of this storm are as follows.

1. VSCS PHAILIN is the most intense cyclone that crossed India coast after Odisha Super Cyclone of 29th October 1999.
2. There was rapid intensification of the system from 10th October morning to 11th October morning leading to an increase in wind speed from 45 knots to 115 knots.
3. At the time of landfall on 12th October, maximum sustained surface wind (MSW) speed in association with the cyclone was about 115 knots (215 kmph) and estimated central pressure was 940 hPa with pressure drop of 66 hPa at the center compared to surroundings.
4. It caused very heavy to extremely heavy rainfall over Odisha leading to floods, and strong gale wind leading to large-scale structural damage and storm surge leading to coastal inundation over Odisha.
5. Maximum rainfall occurred over northeast sector of the system centre at the time of landfall.
6. Based on post-cyclone survey report, maximum of storm surge of 2–2.5 m above the astronomical tide has been estimated in the low lying areas of Ganjam district of Odisha in association with the cyclone and the in-land inundation of saline water extended up to about 1 km from the coast.
7. It caused large-scale damage to property and loss of some human lives.

3. *Model description and configuration*

The WRF-ARW model is developed at the National Center for Atmospheric Research (NCAR) in collaboration with a number of agencies viz., the National Oceanic and Atmospheric Administration (NOAA), the National Center for Environmental Prediction (NCEP) and various universities. It is based on an Eulerian solver for the fully compressible non-hydrostatic equations with complete Coriolis and curvature terms. The model uses the terrain-following hybrid sigma-pressure as vertical coordinate. The grid staggering is the Arakawa C-grid. The solver uses the 2nd and 3rd order Runge–Kutta time integration scheme and 2nd to 6th order advection in both horizontal and vertical directions and time-splitting technique for using smaller time steps for acoustic and gravity-wave modes (Skamarock *et al*. 2008). It also encompasses a number of physical

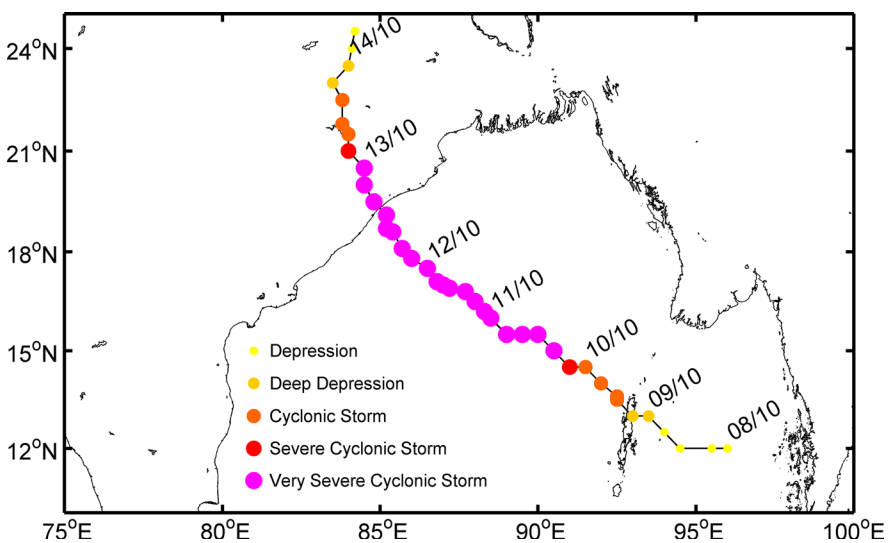

Figure 1
The IMD best-fit track of the Bay of Bengal cyclone 'Phailin' during 08–14 October 2013

parameterization schemes, initialization option and data assimilation packages. A detailed description of the model is provided in Skamarock *et al*. (2008).

The double-nested two-way interactive WRF-ARW model with 27 and 9 km horizontal resolutions customized at IITKGP through extensive sensitivity is used in predicting the cyclonic storm 'Phailin'. The model domains with topography are shown in Fig. 2. There are 35 vertical sigma levels with higher resolution in the boundary layer (BL) with the model top at 10 hPa. The physical parameterization schemes used are old Simplified Arakawa-Schubert (SAS) cumulus scheme (Pan and Wu 1995), Yonsei University (YSU) PBL scheme (Hong *et al*. 2006); Lin microphysics scheme (Lin *et al*. 1983); the Rapid Radiative Transfer Model (RRTM) for longwave radiation (Mlawer *et al*. 1997) and Dudhia's scheme (Dudhia 1989) for shortwave radiation. The overview of the model used in the present study is given in Table 1.

Table 1

Overview of WRF-ARW model configuration

Dynamics	Non-hydrostatic
Model domain	6°S–32.5°N, 66°E–110°E (D1) 0.5°N–26.5°N, 72°E–102°E (D2)
Horizontal grid distance	27 km (D1) and 9 km (D2)
No. of vertical levels	35
Integration time step	60 s (D1), 20 s (D2)
Time integration scheme	Runge–Kutta 3rd order
Map projection	Mercator
Horizontal grid system	Arakawa C-grid
Spatial differencing scheme	6th order center differencing
Radiation parameterization schemes	LW-RRTM SW-Dudhia scheme
Land surface model	Unified Noah LSM
PBL scheme	YSU
Microphysics	Lin
Cumulus parameterization	Old simplified Arakawa–Schubert (SAS4)

4. Numerical experiments and data used

In order to evaluate the performance of the model, five model predictions are generated with different initial conditions beginning at 12 UTC of 08th October, 2013. The five model predictions with the initial condition of 12 UTC of 08th Oct, 00 UTC of 09th Oct, 12 UTC of 09th Oct, 00 UTC of 10th Oct and 12 UTC of 10th Oct will hereafter be referred as E1, E2, E3, E4 and E5. The model configuration is kept unchanged for all the five forecasts generated. The topography for the double-nested model domains are derived from United States Geographical Survey (USGS) global topography datasets at 10- and 5-min resolutions, respectively. The initial condition for the model prediction is derived from NCEP-GFS analysis available at 0.5° × 0.5° resolution. The time-varying lateral boundary conditions are derived from NCEP-GFS forecast and updated in every 3 h. The best-fit track data obtained from India Meteorological Department (IMD) is used for the validation of model-predicted track, intensity and landfall (time and position) of the storm. The performance of the customized model is also compared to that of other NWP models viz., Multi-Model Ensembles (MME), Hurricane WRF (HWRF), IMD-GFS, IMD-WRF, GFS (NCEP), UKMO and JMA models as documented by Kotal *et al*. (2013).

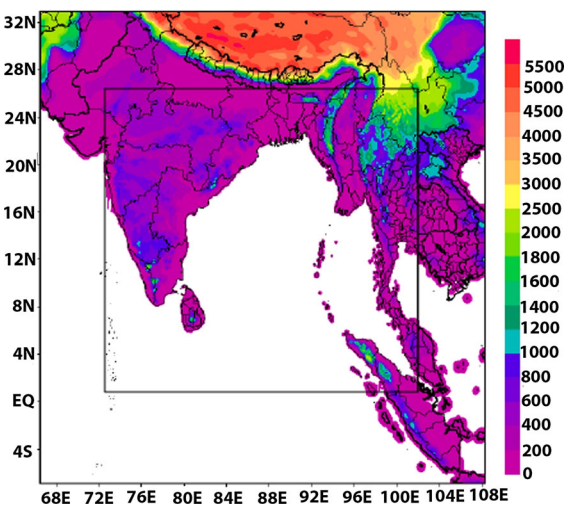

Figure 2
Model domain used in the study with topography

5. Initial conditions

The initial intensity of the storm in terms of CSLP, MSWS and initial positional error are derived from the GFS analysis and IMD best-fit datasets for the five forecast experiments as shown in Table 2. It

Table 2

CSLP, MSW derived from GFS analysis and IMD best-fit datasets and initial positional error at different model initialization time

Initialized time	IMD best-fit data			GFS analysis		
	CSLP (hPa)	MSW (m/s)	Stage (Saffir–Simpson scale)	CSLP (hPa)	MSW (m/s)	Initial positional error (km)
08OCT_12UTC	1003	13	D	1001	20	172
09OCT_00UTC	1002	15	DD	1000	20	74
09OCT_12UTC	999	18	CS	999	22	80
10OCT_00UTC	996	23	CS	987	28	18
10OCT_12UTC	976	38	VSCS	970	48	49

shows that initial intensity of the storm in terms of MSWS derived from GFS analysis are slightly intense than IMD best-fit datasets for all five corresponding initial conditions. The initial positional error is derived as the distance between the initialized storm location from the GFS analysis and IMD best track location. The initial position error gradually decreases with time except E5 and the least initial position error is 18 km for E4 initial condition. It is observed from Table 2 that E3 (09OCT_12UTC) initial condition has less initial intensity error both in terms of CSLP and MSW. Figure 3 shows the Phailin cyclone track derived from GFS analysis and IMD best-fit datasets. The colored marks indicate the location of storm center for respective experiments as derived from MCSLP. It is very clear that the GFS analysis produces the storm which closely follows the observed track, but with large displacement error at the incipient stage of the storm viz., at 12 UTC of 08th OCT 2013.

6. Results and discussion

The evaluation of the performance of the customized WRF-ARW model in real-time prediction of the VSCS 'Phailin' is mainly focused on track, time and location of landfall, intensity and rainfall associated with the storm. The analysis of model simulated storm inner-core structure and dynamics are not carried in the study, since the model resolution (9 km) is not sufficient enough to resolve such features (Davis *et al*. 2008). Model-predicted mean vector displacement error (VDE) and error in landfall time and location are compared with that of the other NWP models. The model-predicted intensity in terms of CSLP and MSW is compared with IMD best-fit track datasets. The predicted rain rate is compared with satellite-derived rain rate and station observations. The results are presented and discussed in following sub-sections.

6.1. Track

Figure 4 shows the tracks of VSCS 'Phailin' obtained from model predictions along with IMD best-fit track. In all the five forecasts [E1, E2, E3, E4 and E5] the model-predicted track follows the observed track throughout the forecast period with the predicted track to the left of the observed track in the first 48 h and right of it in the next 48 h. Table 3 summarizes the errors in all the five model predictions. The experiment E1 with 12:00 UTC of 08th October initial condition has the earliest landfall among the five predictions with a large landfall time error of 10 h compared to observed landfall. E2, E3, E4 and E5 accounted lesser landfall time error and with E4 providing accurate landfall time at 17:00 UTC of 12 October and minimum landfall position error of 18 km. Experiment E3 with 12 UTC of 09th October initial condition is found to have the second least landfall position error of about 32 km away to the right of the actual landfall position. The forecast experiment E4 with least initial positional error (described in Sect. 5) has least landfall positional error with time of landfall exactly matches with observation. It is noted that though E5 also have very less landfall time error, but has maximum landfall positional error of 114 km. In addition to landfall, the mean vector displacement error is also less for E3

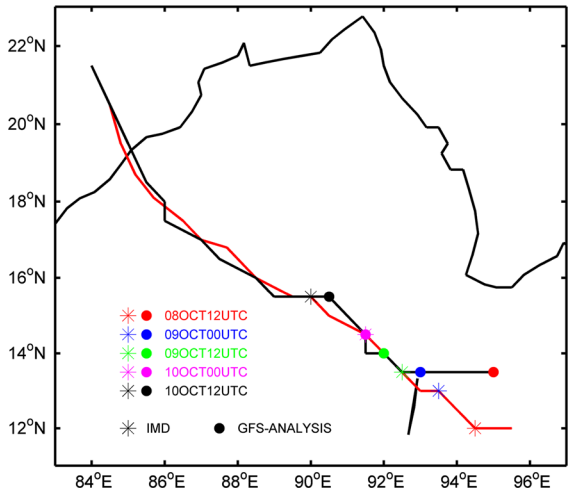

Figure 3
Phailin track derived from GFS analyses and IMD best-fit data with the initial position of the storm in the five forecast experiments

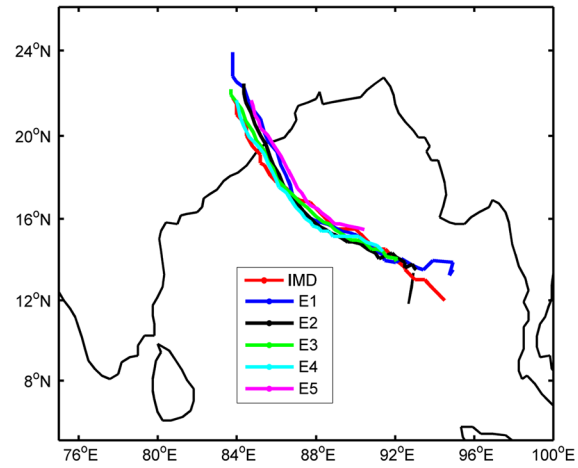

Figure 4
The IMD best-fit and model-predicted tracks of 'Phailin' cyclone with different initial conditions

(44 km) and E4 (48 km) compared to other forecast experiments. This clearly indicates that the landfall position and time of the storm is better predicted if the initial position of the storm is specified accurately.

Figure 5 presents the translation speed of the storm derived at 12 h interval from five model predictions and IMD best-fit track data. In E1 the translation speed of the storm is significantly higher than that of observed storm throughout the forecast period, leading to very early landfall. In other experiments (E2–E5), the translation speed of the storm is similar and slightly higher than that of the observed storm during the intense period but differs significantly in the early stages. The model predictions E1 and E2 which has increased translation speed are associated with over-prediction of storm intensity. Figure 6 displays the VDEs for the five model forecasts at 12 h interval. It reveals that experiments E3 and E4 with less initial errors (position and intensity) have less VDE compared to other forecasts especially in first 72 h. The mean VDEs of all the five forecasts range in 50–70 km during first 72 h. The results indicate that the customized WRF-ARW is able to predict the track of the storm quite accurately, particularly with 00:00 UTC 10 October initial condition.

The mean VDEs of the five forecasts using customized WRF-ARW and errors in other NWP forecasts including IMD official forecast are presented in Fig. 7. The mean VDEs of E3 and E4 are also presented. It clearly indicates that VDEs in the customized WRF-ARW forecast is consistently less compared to the other NWP models as well as IMD official forecast, except in 36 h forecast. It should be noted that the average track forecast error was highest in IMD-WRF with mean displacement of 95 km at 12 h to 265 km at 72 h forecast and also the error in the JMA track forecasts are about 85 km at 12 h to 254 km at 72 h. The mean track errors in IMD-MME, NCEP-GFS and UKMO are approximately of the same order and are about 65 km at 12 h to 104 km at 60 h forecasts, respectively. In the IMD-HWRF, the errors are about 49 km at 12 h and 183 km at 60 h forecasts, respectively. In IMD official forecast, the errors are about 63 km at 12 h and 90 km at 60 h forecasts, respectively. The steering current vector (SCV) around the storm is computed using NCEP FNL analysis at every 6 h during 00:00 UTC 08 October to 00:00 UTC 13 October. The horizontal mean winds within 1.5°–7° radius of the storm are calculated in the levels between 925 and 200 hPa and are given the variable weights based on maximum potential vorticity at that level to estimate the SCV. The comparison of the SCVs with the storm track indicates that the storm followed the steering current (figure not presented). This has possibly led to reasonably accurate prediction of the track of the storm by the model.

Table 3

Model forecast error in landfall (time and location), mean VDEs over the whole period of the forecast and peak intensity (in terms of CSLP and MSW) obtained from five forecast experiments and IMD best-fit datasets

	IMD (best fit)	E1	E2	E3	E4	E5
Landfall time error (h)	–	10	2	4	0	1
Landfall positional error (km)	–	92	63	32	18	114
Mean vector displacement error	–	151	59	44	48	71
Max wind speed at peak intense stage (m/s)	59	49	51	48	48	48
Min CSLP at peak intense stage (hPa)	940	934	932	939	946	942

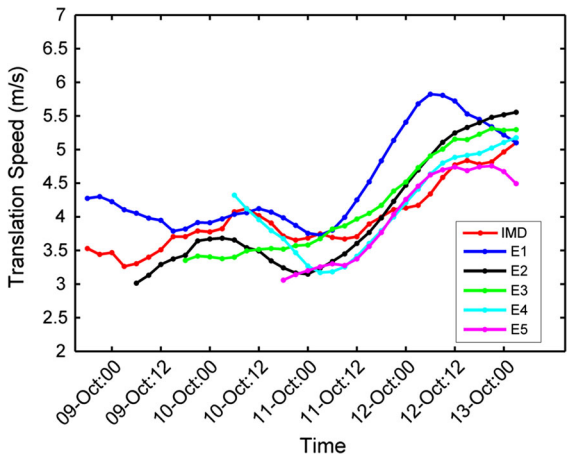

Figure 5
Translation speed of the storm derived from five model predictions and IMD best-fit track data at 12-h intervals

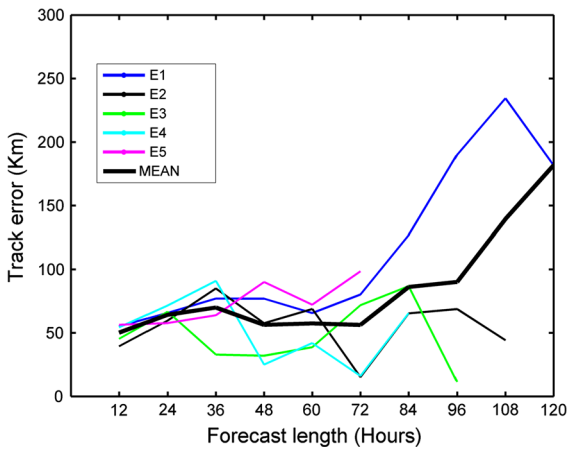

Figure 6
VDEs in model prediction in reference to the best-fit track with different initial conditions

6.2. *Landfall*

Figure 8 presents reflectivity predicted by the model in E3 and E4 and the reflectivity from DWR at Vishakhapatnam valid at 15:00, 16:00 and 17:00 UTC of 12 October 2013, i.e., around the actual landfall time of the storm. The landfall in these two forecasts is discussed in this section as they provided better prediction of the storm. The landfall errors in other experiments are already discussed in Sect. 6.1. This clearly shows that the landfall time of the storm predicted by the model with 00:00 UTC 10 October initial condition exactly matches with the observation and the location of landfall is also predicted quite accurately (18 km away). With initial condition of 12:00 UTC 09 October, the model could not predict the landfall accurately. The landfall time is 4 h before the actual landfall time and the location of landfall is 32 km away from the observed landfall location.

The mean errors in forecasting the landfall position and time by different NWP models are provided in Table 4. It is observed that HWRF and UKMO models have always (with all different initial condition) predicted landfall to the right of actual landfall point (figure not presented) with maximum error of 340 km in HWRF forecast. The IMD-GFS and NCEP-GFS have predicted landfall sometimes to the right and sometimes to the left depending on the initial condition. The JMA and WRF-VAR have always predicted landfall to the left with a maximum limit of about 215 km (Kotal *et al.* 2013). The table also shows that only IMD-MME and customized WRF-ARW model could predict landfall point near Gopalpur with errors

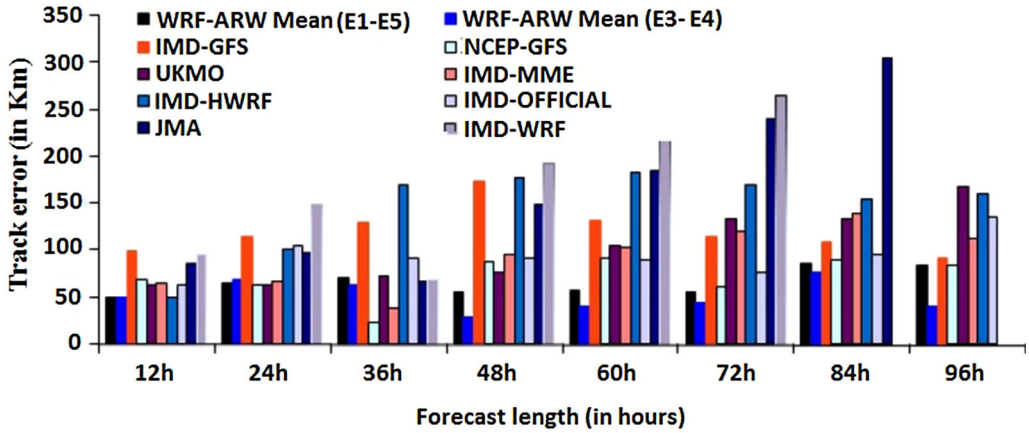

Figure 7
Mean VDEs of all five and two (E3 and E4) model forecasts along with other NWP model forecast with different lead time

(mean) of 20 km and 25 (mean of E3 and E4) km, respectively. The mean of landfall location errors in the five forecasts with customized WRF-ARW model is 65 km. This is mainly due to large landfall position error in E1 and E4. The maximum predicted landfall position error is about 144 km in IMD-HWRF model. Most of the models predicted delayed landfall except NCEP-GFS which predicted advance landfall. The mean absolute landfall time errors in different models are also provided in Table 4. This indicates that IMD-MME and the customized WRF-ARW model used in this study provided better forecast of landfall time as well.

6.3. *Intensity*

The time evolution of observed and model-predicted intensity of the storm in terms of CSLP is shown in Fig. 9. The model-predicted intensity of the storm in terms of CSLP in all five forecasts follows the observed trend of intensification. However, model forecasts E1 and E2, initialized at very less intense stage (D and DD), have over-predicted the peak storm intensity. In E2 forecast, the storm dissipated early as it undergoes early landfall due to increased translation speed. In E3 forecasts, the intensity of the storm follows the observed intensity throughout the forecast period. Also the mean predicted intensity of the storm (in terms of CSLP) from all five forecasts followed the observed intensity.

The intensity of the storm (in terms of MSW) obtained from model forecasts and IMD best-fit data is presented in Fig. 10. Though the model is initialized with slightly higher intensity of the storm (as derived from GFS) in all the experiments as seen in Sect. 5, the MSW is under-predicted after 40 h of model integration in all five forecasts. The mean peak MSW of all five forecasts is about 49 m/s, which is almost 10 m/s lower than actual peak MSW of the storm. The velocity fields are usually under-predicted by the NWP models, particularly in the tropical region due to erroneous winds in the analysis over the region. The erroneous velocity field in the tropical analysis is due to domination of mass fields in the observations compared to that of the velocity fields. Considering this limitation in NWP guidance with respect to MSW, model-predicted CSLP is used to estimate MSW based on Mishra and Gupta (1976) formulation for NIO region as shown in Eq. (1).

$$\mathrm{MSW} = 14.2 \times \sqrt{p_o - \mathrm{CSLP}}, \qquad (1)$$

where p_o is the outermost closed isobar.

Figure 11 presents the estimated MSW from the model-predicted CSLP in all the forecast experiments. The trend of sharp intensification and dissipation of the storm after landfall is well captured by the model, and in particular E3 follows the observed trend very closely. The peak intensity was maintained up to 15:00 UTC 12 October as

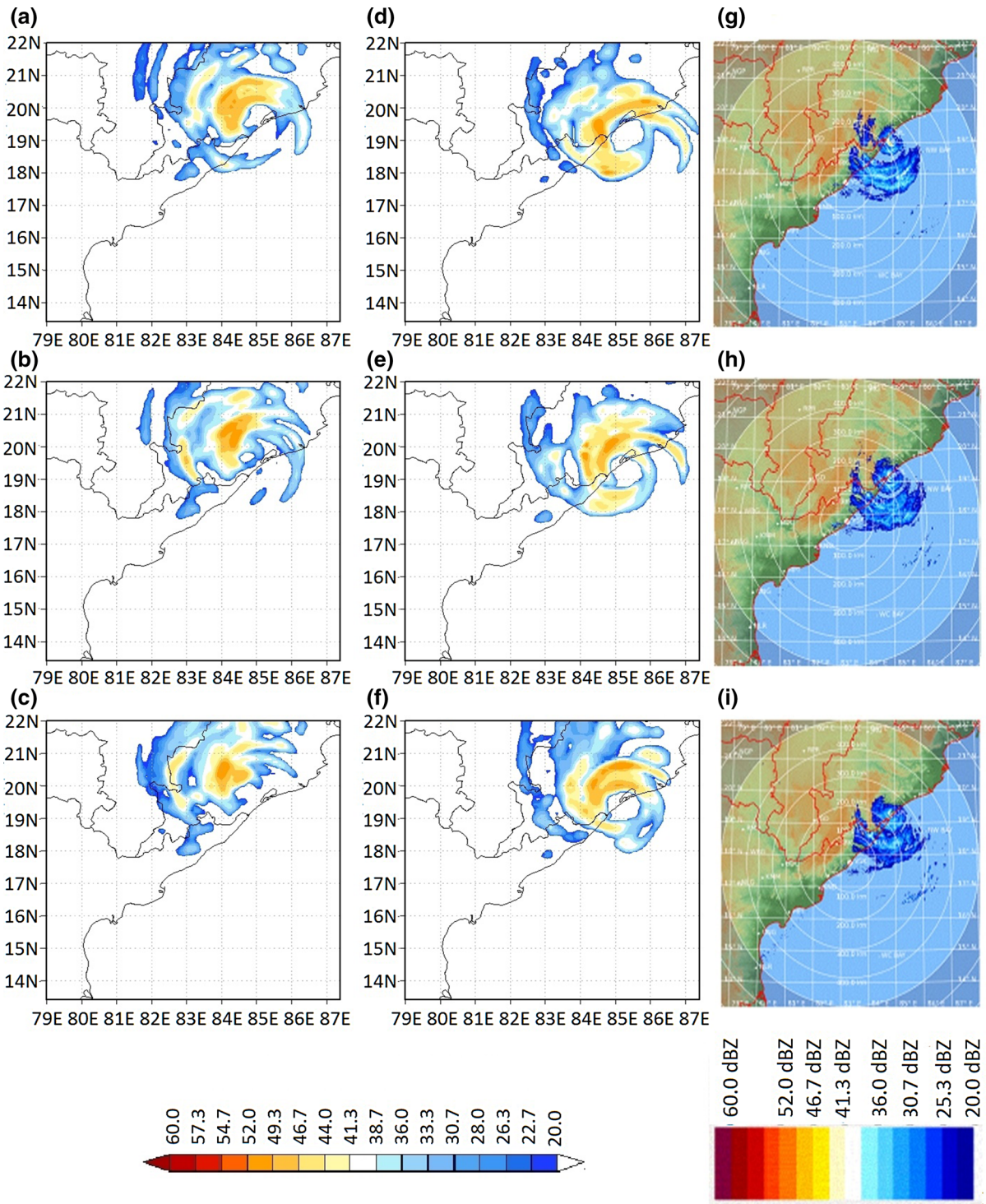

Figure 8
Model-predicted and DWR maximum reflectivity at 15:00 UTC, 16:00 UTC and 17:00 UTC; *left panel* predicted with E3 (12:00 UTC 09 October) initial condition, *middle panel* predicted with E4 (00:00 UTC 10 October) initial condition and *right panel* from Vishakhapatnam DWR

Table 4

The mean landfall position and time errors obtained from WRF-ARW forecasts and other NWP model forecasts

S. no.	NWP models	Mean landfall errors	
		Position (in km)	Time (in h)
1.	IMD-MME	20	1.9
2.	NCEP-GFS	36	2.9
3.	IMD-GFS	41	6.6
4.	UKMO	44	2.4
5.	WRF-ARW (mean of 5 forecasts)	63	3.4
6.	WRF-ARW (mean of E3 and E4)	25	2
7.	IMD-WRF	69	10
8.	JMA	73	2.3
9.	IMD-HWRF	144	3.9

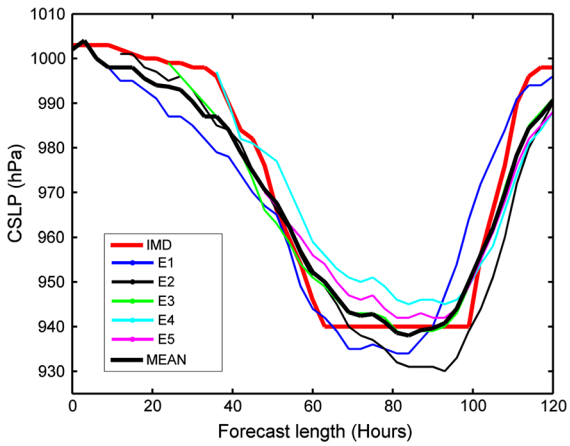

Figure 9
Temporal variation in intensity (with different initial conditions) in terms of observed and model-predicted CSLP

observed from IMD best-fit dataset. Table 3 shows the MSW and CSLP at peak intense stage of the storm in all five forecast experiments. It shows that E3 has captured the peak intensity of the storm with 939 hPa CSLP and 60 m/s MSW at 12 UTC 11 October. Table 5 shows the mean absolute errors in intensity in terms of estimated MSW in all five experiments and the best forecast experiment E3 with other NWP model forecasts. It shows that the mean absolute error in intensity forecast by the customized WRF-ARW model is significantly less than that of in IMD-SCIP, IMD-HWRF and IMD-OFFICIAL. In IMD-OFFICIAL forecast the errors in 24, 36 and 48 h intensity forecasts are 14.9, 18.7

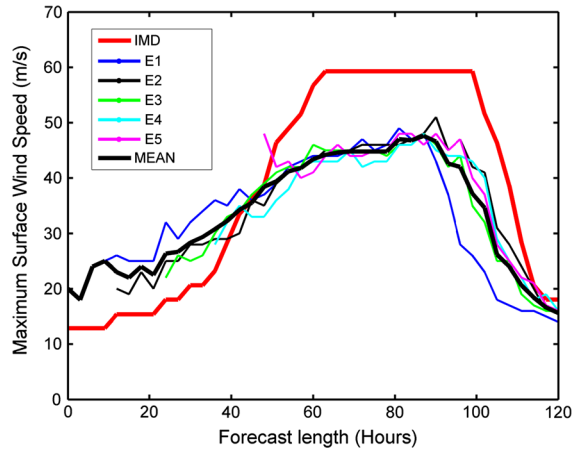

Figure 10
Temporal variation in intensity (with different initial conditions) in terms of observed and model-predicted MSW

and 11.1 m/s, respectively, while the mean errors in the customized WRF-ARW forecasts are 8.3, 2.9 and 4.8 m/s.

The results discussed above indicate that the intensity of the storm in terms of CSLP is well predicted but the same is under-predicted in terms of MSW; however, the estimated MSW (from predicted CSLP) provides a better intensity forecast in all five experiments.

6.4. *Potential vorticity and vertical wind shear*

As discussed in previous sections, the model forecasts E1 and E2 initialized with CSLP of 1001 and 1000 hPa respectively over-predicted the peak intensity of the storm. The forecast E3 is initialized with initial intensity (CSLP) same as observed has better predicted the trend of intensification, peak intensity and dissipation. In E4 and E5, the model is initialized with intensity slightly higher than the actual intensity of the storm, while the peak intensity is slightly under-predicted by the model. In this section, the predicted intensity of the storm in all the five model forecasts is discussed in the context of Potential Vorticity (PV) and Vertical Wind Shear (VWS). The feedback of latent heating on atmosphere dynamics has a greater impact on cyclone evolution. Potential vorticity is a non-conserved quantity in the presence of diabatic heating (latent

heat), which makes it an indicator of the impact of latent heating in the atmosphere. The rate of PV generation or destruction is completely determined by the magnitude and gradient of the latent heating and the magnitude of the absolute vorticity (STOELINGA 1996). The vertical distribution of PV provides a clear indication of optimum environmental steering current associated with storm motion (SINGH *et al.* 2012).

$$\mathrm{PV} = -g(\xi_\theta + f)\frac{\partial \theta}{\partial \mathrm{P}}, \qquad (2)$$

where 'g' is the acceleration due to gravity; 'ξ_θ' is the horizontal relative vorticity; 'f' is the Coriolis parameter and 'θ' is the potential temperature. PV is estimated from GFS analysis using the above Eq. (2) and the vertical profile is generated by averaging PV over an annular radius of 1° from storm center. Figure 12 represents the vertical profile of PV derived

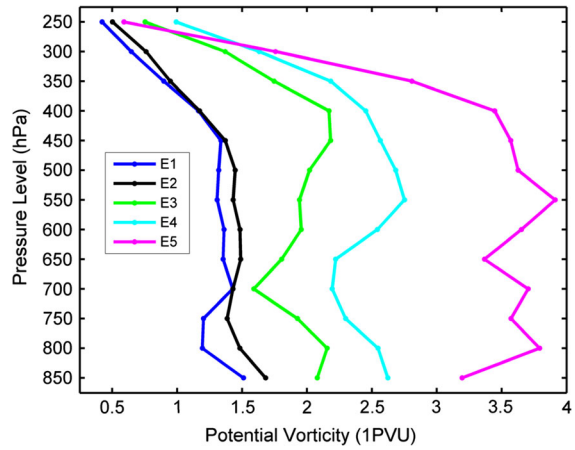

Figure 12
Vertical profile of Potential Vorticity (PV) derived from GFS analyses at different initial conditions. PV is expressed in the units of 1PVU that equals 10^{-6} m^2/K/kg

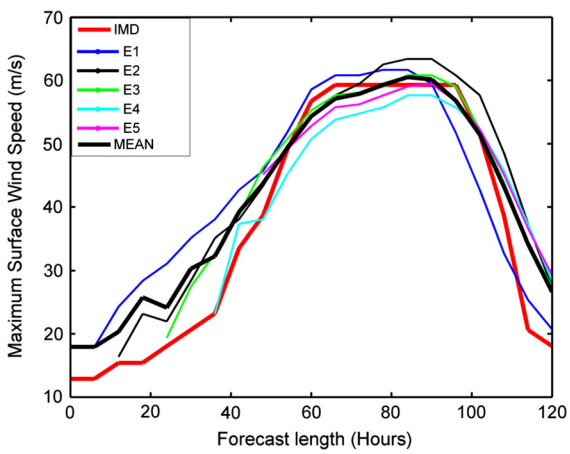

Figure 11
Temporal variation in intensity (with different initial conditions) in terms of observed and MSW estimated from model-predicted pressure drop

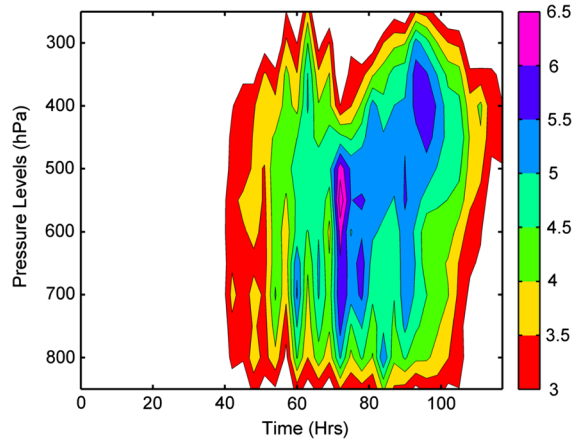

Figure 13
Temporal evolution of vertical distribution of Potential Vorticity (PV) derived from GFS analyses at 3-h time interval. The time axis shows 120-h period that begins from 08OCT_12UTC. PV is expressed in the units of 1PVU that equals 10^{-6} m^2/K/kg

Table 5

Mean intensity error in terms of MSW estimated from WRF-ARW predicted CSLP and other NWP model forecasts

NWP models	Forecast hour									
	12 h	24 h	36 h	48 h	60 h	72 h	84 h	96 h	108 h	120 h
WRF-ARW (E1–E5 mean)	5.3 (5)	8.3 (5)	5.1 (5)	2.9 (5)	2.7 (5)	4.8 (5)	4.8 (4)	8.9 (3)	7.6 (2)	2.6 (1)
WRF-ARW (E3–E4 mean)	5.0 (2)	6.8 (2)	2.9 (2)	1.4 (2)	2.5 (2)	3.6 (2)	7.7 (2)	–	–	–
IMD-SCIP	10.4 (8)	18.3 (7)	23.7 (6)	24.6 (5)	31.5 (4)	36.7 (3)	–	–	–	–
IMD-HWRF	17.0 (6)	21.0 (5)	27.8 (5)	30.5 (4)	28.3 (3)	19.5 (2)	11.0 (1)	–	–	–
IMD-OFFICIAL	9.1	14.9	17.4	18.7	17.7	11.1	19.7	10.5	1.8	5.4

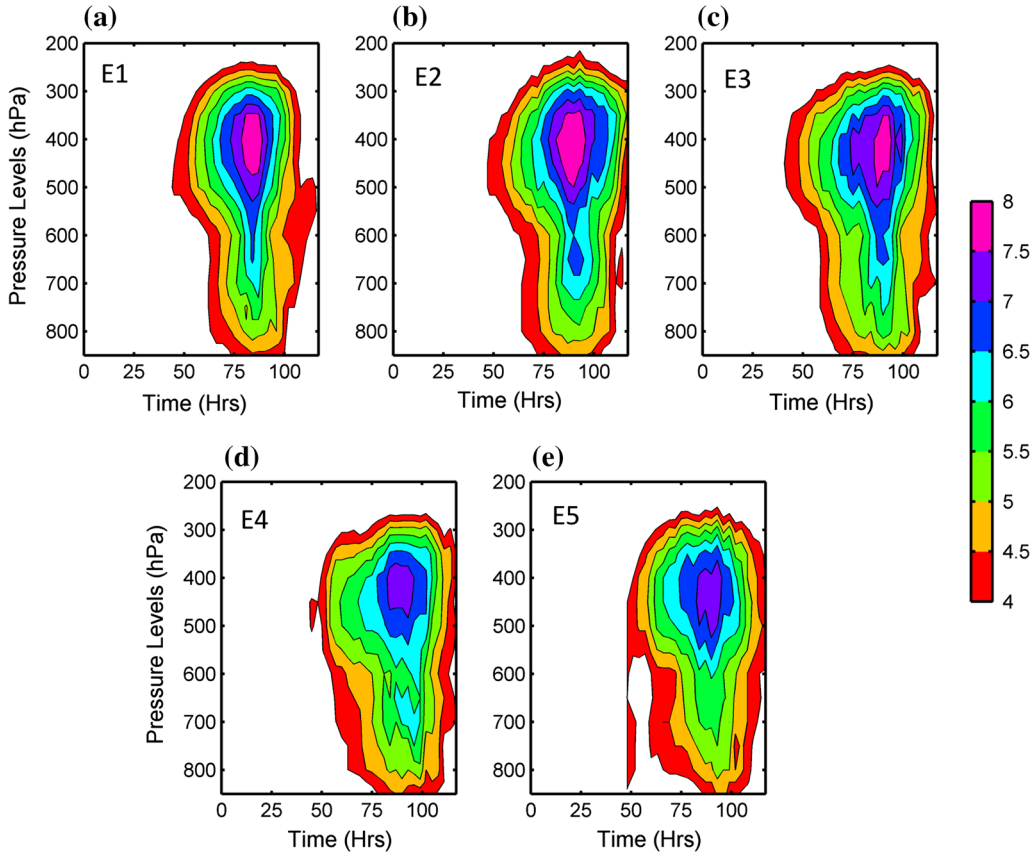

Figure 14
Temporal evolution of vertical distribution of Potential Vorticity (PV) derived from model simulations at 3-h time interval. The time axes show 120-h model simulation period that begins from 08OCT_12UTC. PV is expressed in the units of 1PVU that equals 10^{-6} m^2/K/kg

from the GFS analysis for the five initial conditions and PV is expressed in the units of 1PVU that equals 10^{-6} m^2/K/kg. The increase in PV around the storm is clearly seen as the intensity of the storm in GFS analysis increases in the successive initial conditions. PV profile corresponding to E1 and E2 indicates a maximum value at 850 hPa (nearly 1.5 and 1.7 PVU) and a near uniform PV distribution is observed in the middle troposphere between 700 and 400 hPa. This PV maximum is due to higher absolute vorticity at that level.

In E3 and E4 initial conditions the primary PV maxima is observed between 850 and 800 hPa, the secondary maximum in E3 and E4 is observed around 550 and 450 hPa, respectively. The primary maximum is due to absolute vorticity at that level, whereas secondary maximum is due to generation of latent heat associated with cloud condensation process. This corroborates with the findings of Brennan *et al.* (2008) who has analyzed the secondary PV in a well-organized cyclogenesis. It should be noted that the level of PV maxima in E4 and E5 initial conditions are comparatively lower (550 hPa) leading to under-prediction in peak intensity of the storm.

In GFS analysis, the storm reached peak intensity of 85 m/s at 12 UTC of 12th October, 2013. Figure 13 presents evolution of vertical distribution of PV during the period 12 UTC of 8th October and 09 UTC of 13th October derived from 3 hourly GFS analysis. The peak intense stage of the storm in the GFS is in conjunction with mid-tropospheric PV maxima, which is associated with enhanced latent heating of the atmosphere. This clearly indicates that the storm reached its peak intensity when the secondary PV maximum (6 PVU) is around 400 hPa.

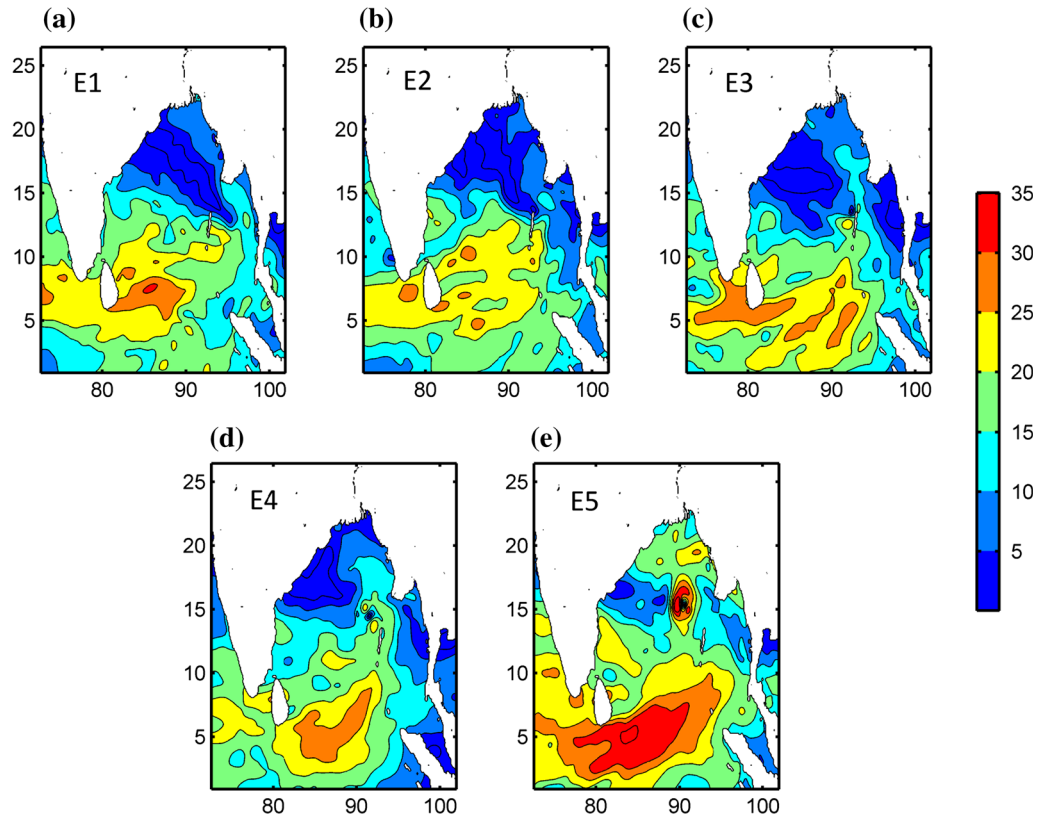

Figure 15
Vertical wind shear at different initial conditions derived from GFS analyses. The unit of vertical wind shear is m/s

Figure 14 illustrates the evolution of vertical distribution of PV in five model forecasts. In E1, E2 and E3 the magnitude of secondary PV maxima is 8 PVU with the level of maxima is slightly lower (~420 hPa) in E3 compared to E1 and E2. The level of secondary PV is highest (~400 hPa) in E2. In E4 and E5, the magnitude of secondary PV maximum is less and also at lower level compared to that of the other forecast experiments. It may be mentioned here that the peak intensity of the storm is over-predicted in E1 and E2 with more over-prediction in E2. The peak intensity was better predicted in E3 and under-predicted in E4 and E5. This clearly indicates that the intensity of the storm is closely linked to not only to the magnitude of secondary PV maxima, but also its level of occurrence.

Figure 15 shows the vertical wind shear (VWS) derived from GFS analysis at the time of initialization of the five model forecasts. VWS is estimated using the following Eq. (3).

$$\mathrm{VWS} = \sqrt{|U_{200} - U_{850}|^2 + |V_{200} - V_{850}|^2}, \qquad (3)$$

where U_{200} and V_{200} is the zonal and meridional wind components, respectively, at 200 hPa; U_{850} and V_{850} is the zonal and meridional wind components, respectively, at 850 hPa.

The distribution of VWS is similar in E1 and E2 initial conditions with weaker VWS around the storm environment in E2. In E3 initial condition, VWS is slightly stronger than that of E1 and E2. As discussed in Sect. 6.3, the intensity of the storm is well predicted in E3 and over-predicted in E1 and E2. In E4 and E5 initial conditions, VWS is significantly stronger that led to under-prediction of storm intensity. This indicates that the intensity forecast of the model depends on VWS around the storm in the initial condition.

6.5. Rapid intensification

In this section, analysis of E3 and E4 forecasts are presented as they provides better forecasts of the storm compared to the other experiments. Hence the analysis is restricted to E3 and E4 in the current and following section. As observed, the storm intensified sharply between 00:00 UTC of 10 October and 03:00 UTC of 11 October 2013 during which the pressure dropped by 56 hPa. In the forecasts also the sharp intensification of the storm takes place during this period but the rate of intensification is not as sharp as observed and the intensification continued at a slower rate for some more time. In the model forecasts E3 and E4 with 12:00 UTC 09 October and 00:00 UTC 10 October initial conditions, the CSLP dropped by 38 and 40 hPa, respectively, during 00:00 UTC of 10 October to 03:00 UTC of 11 October 2013. Figure 16 presents the observed (best-fit) and forecasted tracks of the storm superimposed over Tropical Cyclone Heat Potential (TCHP) computed following the methodology proposed by Balaji and Mandal (2014). This clearly shows that the storm intensified sharply during this period as it passed over the higher TCHP zone with an average of 75 kJ cm^2 around the storm path.

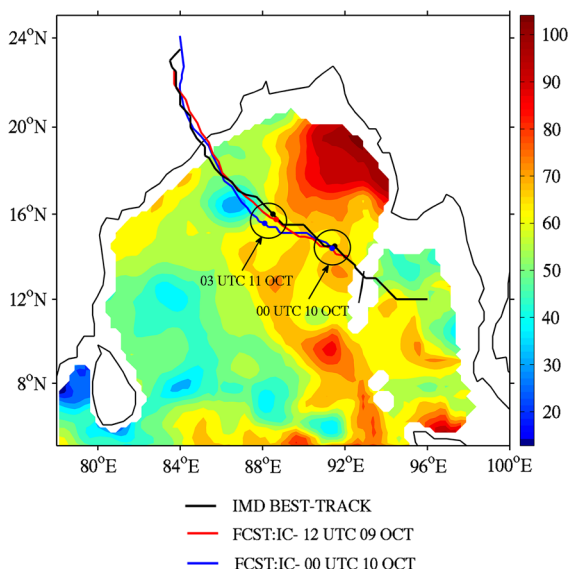

Figure 16
The IMD best-fit track and model-predicted best track of E3 and E4 forecast superimposed over TCHP of 08 October 2013

6.6. Precipitation

Similar to previous section, the results from E3 and E4 are discussed. Figure 17 shows rainfall rate (in inches/h) valid at 00:00UTC 12 October from model forecasts and derived from SSMI F-16 and METEO-7. The regions of maximum precipitation and distribution of rain bands in the model predictions (in the south-west sector) matches well with the satellite-derived observation though the magnitude of rain-rate in the core region of the storm is slightly over-predicted. With E3 initial condition, the model over-predicted rainfall in northwest and southeast sector while with E4 initial condition, the over-prediction is only in the southeast sector.

The 24-h accumulated precipitation from E3 and E4 forecasts and observation valid at 03:00 UTC of 13 October is presented in Fig. 18. The observed rainfall presented here are station rainfall over different districts of Odisha. In general, precipitation in most of the districts in Odisha is over-predicted in both forecasts with more over-prediction in E4. The rainfall over central part of coastal Odisha is well predicted. In the forecasts, the maximum precipitation of 400 mm occurred at Banki, Odisha, where observed precipitation was 381 mm. Over-prediction is more pronounced in interior Odisha. The accumulated rainfall is under-predicted in the northeastern part of Odisha in both the forecasts.

Figure 19 illustrates model-predicted 84-h accumulated precipitation during 00:00 UTC 10 October to 12:00 UTC of 13 October with superimposed model-predicted track of E3 and E4. It shows that in both predictions heavier precipitation is to the left of the track over ocean as well as over land. The model-predicted heavier precipitation in south Odisha is in contrast to the observation that recorded more precipitation in north Odisha.

7. Summary

The study evaluates the performance of the customized WRF-ARW model in real-time prediction of Bay of Bengal cyclone ‘Phailin’. Five real-time predictions are generated with five different initial conditions derived from GFS analysis and lateral boundary

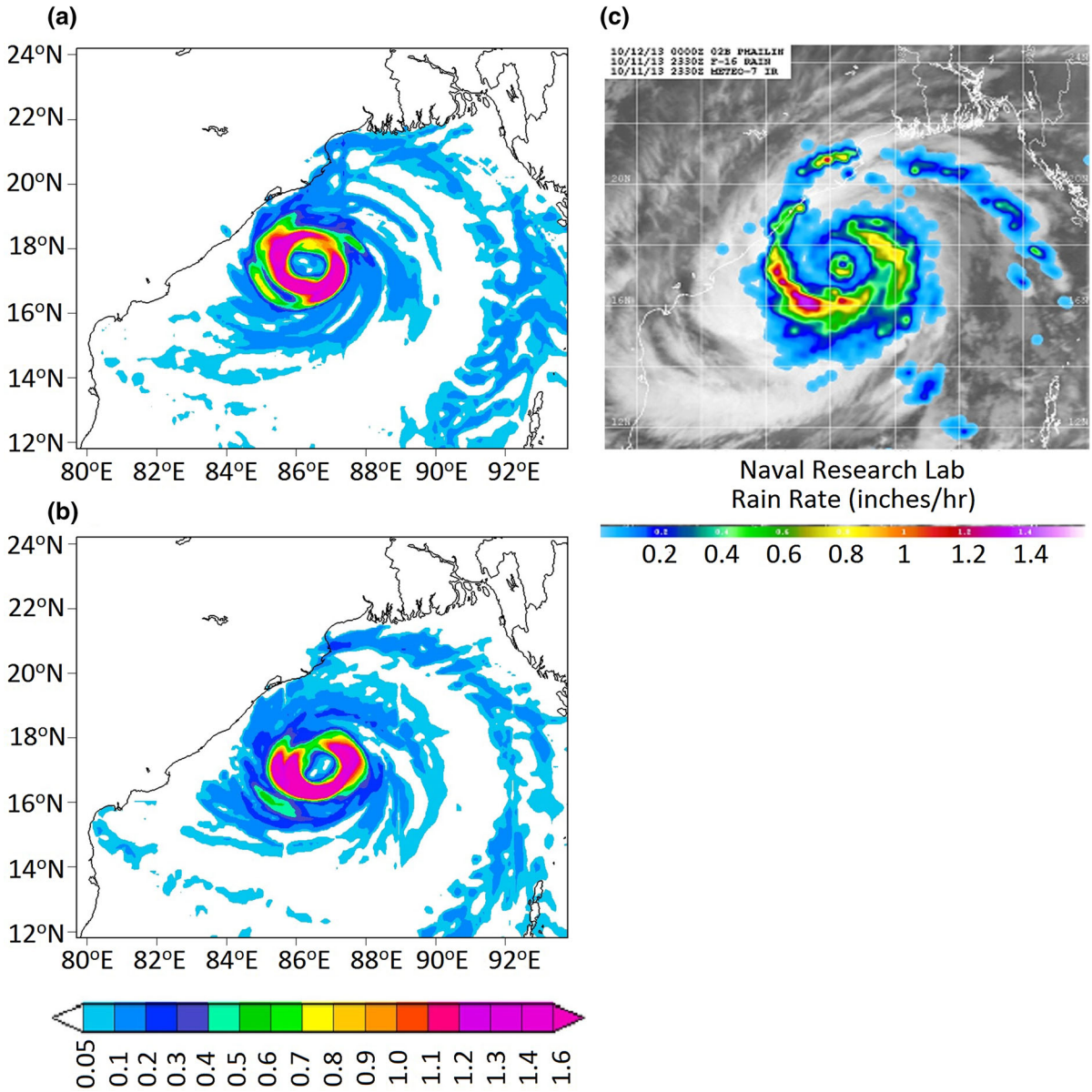

Figure 17
Rainfall rate (in inches/h) valid at 00:00UTC of 12 October in **a** E3 forecast, **b** E4 forecast and **c** derived from SSMI F-16 and METEO-7

condition provided every 3 hourly using GFS forecast. The results are analyzed towards the prediction of track, intensity, landfall (time and position) and associated precipitation. The results presented and discussed in the previous section can be summarized as follows:

The track of the storm is reasonably well predicted by the model with the five different initial conditions. The mean VDEs during the whole period of forecast are varying in the range of range of 44–151 km, where the maximum initial positional error itself was about 172 km. The prediction of track and landfall (time and location) of the storm significantly depends on the initial positional error. The error in predicting landfall time is more if the

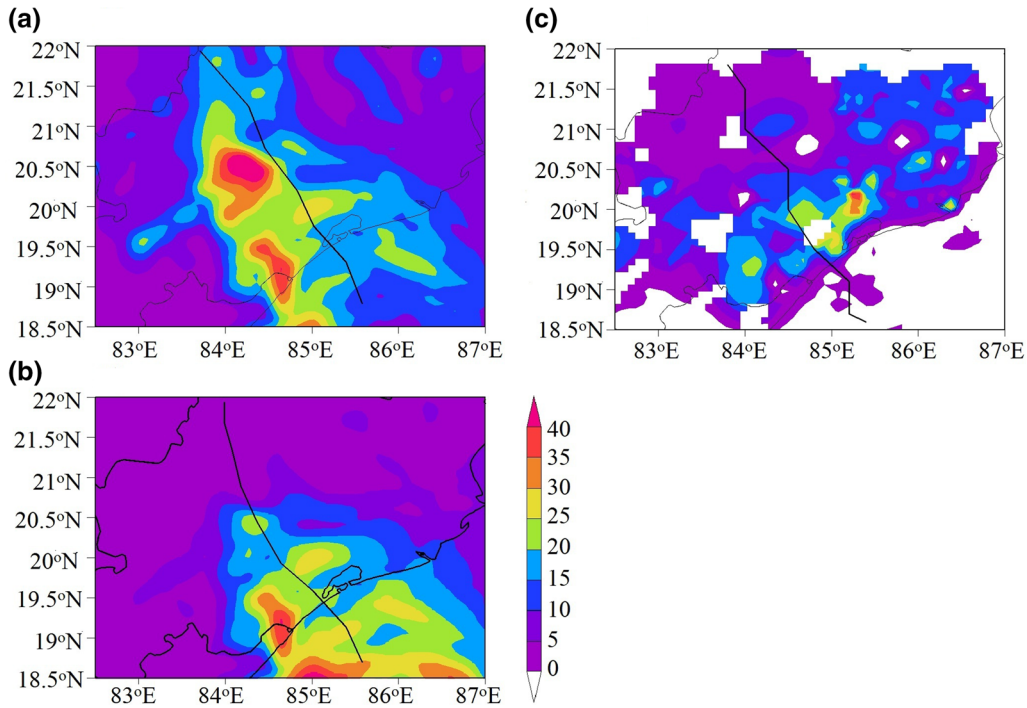

Figure 18
24-h accumulated rainfall valid at 03:00 UTC of 13 October: **a** E3 forecast, **b** E4 forecast, **c** observed station rainfall

translation speed of the storm is higher which is closely associated with over-prediction of storm intensity.

The model-predicted intensity of the storm significantly depends on the stage at which the model has been initialized. The intensity, trends of intensification and dissipation and also the peak intensity of the storm in terms of CSLP is well predicted by the model if initialized at the cyclonic stage. The intensity is over-predicted if the model is initialized at the depression and deep depression stage of the storm and under-predicted if initialized in severe cyclonic stage. The intensity of the storm in terms of MSW is significantly under-predicted by the model at the intense stage of the storm. But MSW estimated from predicted CSLP can well represent the storm intensity.

The rapid intensification of the storm during 00:00 UTC 10 October to 03:00 UTC 11 October is reasonably well predicted by the model and is due to the passage of the storm over the higher TCHP zone. The intensity of the storm is closely associated with vertical distribution of PV. The storm reaches its peak intensity when the level of secondary PV maximum lies between 450 and 400 hPa. The peak intensity of the storm depends not only on the magnitude of secondary PV maxima, but also on the level at which it is observed. The model-predicted intensity of the storm is also significantly influenced by the vertical wind shear in the model initial condition.

The spatial distribution of rain rate associated with the storm at its peak intense stage is reasonably well predicted by the model with over-prediction in core region of the storm. The maximum rain rate in the south-west of the storm as seen in observation is well predicted by the model. Though the precipitation affected regions are reasonably well predicted by the model, the magnitude and distribution of accumulated precipitation is over-predicted (under-predicted) in southern (northern) part of Odisha.

The intensity of the storm is significantly better predicted by the customized WRF-ARW model compared to IMD-SCIP, IMD-HWRF and IMD-

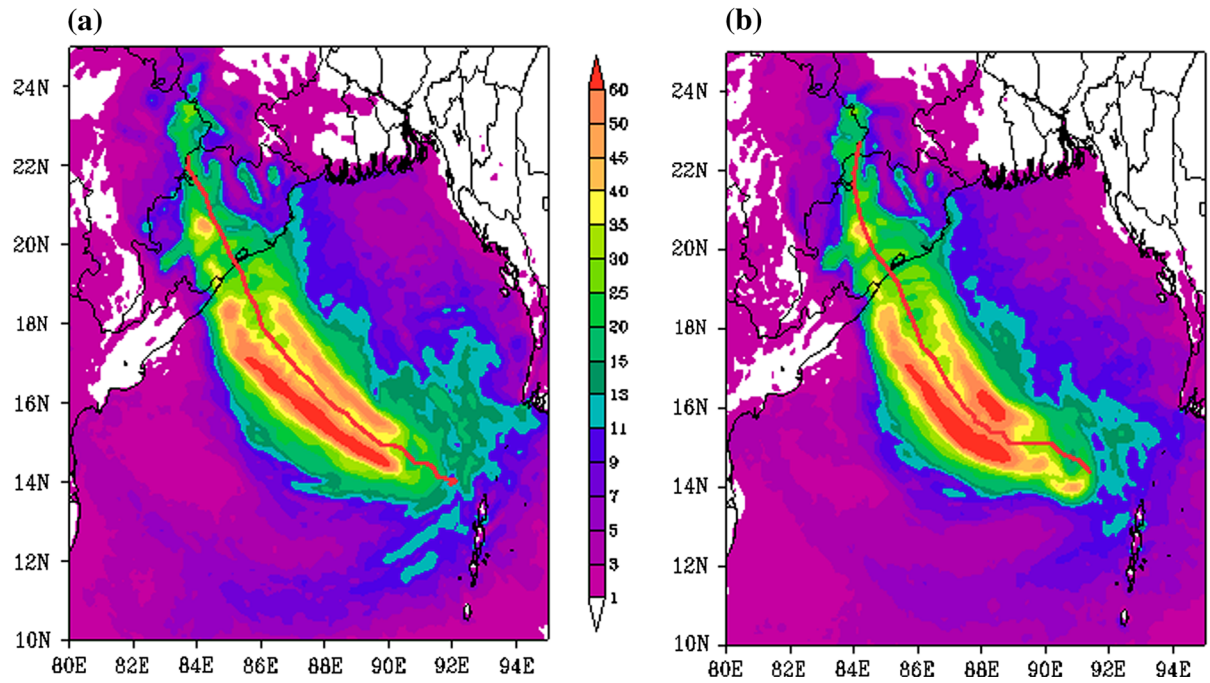

Figure 19
Model-predicted 84-h accumulated precipitation during 00:00 UTC 10 October to 12:00 UTC 13 October with the track of the storm superimposed: **a** E3 forecast, **b** E4 forecast

OFFICIAL. The track of the storm is also better predicted by the model compared to other NWP models, except in 36 h forecast. Reasonably accurate prediction of track of the storm by the NWP models is due to fact that the storm followed the steering current very closely. The mean landfall (position and time) forecast errors of different NWP models indicates that IMD-MME and the customized WRF-ARW model (initialized at CS stage) could predict landfall (position and time) with less error than other NWP models.

Acknowledgments

The authors sincerely acknowledge the IMD for providing the best-fit track data and the DWR reflectivity of the tropical cyclone, NCEP for their GFS analysis and forecast datasets and NCAR for the WRF model. The Council of Scientific and Industrial Research (CSIR) and MoES are acknowledged for funding the research activity.

References

Abhilash, S., Das, S., Kalsi, S.R., Gupta, M.D., Mohankumar, K., George, J.P., Banergee, S.K., Thampi, S.B., and Pradhan, D. (2007), *Impact of doppler radar wind in simulating the intensity and propagation of rain bands associated with mesoscale convective complexes using MM5-3DVAR system*, Pure appl. geophys. *164*, 1491–1509. DOI 10.1007/s00024-007-0235-2.

Balaji, M., and Mandal, M. (2014), Representation of upper ocean heat content in numerical model for prediction of tropical cyclones: An analysis, Ocean Modeling. (Communicated).

Bhashkar Rao, D.V., and Prasad D.H. (2006), *Numerical prediction of the Orissa super cyclone (1999): Sensitivity to the parameterization of convection, boundary layer and explicit moisture processes*", Mausam. *57*(1), 61–78.

Bhashkar rao, D.V., Hari prasad, D., Srinivas, D, and Anjaneyulu, Y. (2010), *Role of vertical resolution in numerical models towards the intensification, structure and track of tropical cyclones*, Marine Geodesy. *33*, 338–355.

Brennan, M. J., G. M. Lackmann, and K. M. Mahoney. (2008): *Potential vorticity (PV) thinking in operations: The utility of non-conservation*. Wea. Forecasting, *23*, 168–182.

Davis, C., Wang, W., Chen, S.S., Chen, Y., Kristen, C., Mark, D., Dudhia, J., Holland, G., Klemp, J., Michalakes, J., Reeves, H., Rotunno, R., Snyder, C., and Xiao, Q. (2008), *Prediction of landfalling hurricanes with the advanced hurricane WRF Model*, Mon. Wea. Rev. *136*, 1990–2005.

Deshpande, M. S., Pattnaik, S., and Salvekar, P.S. (2010), *Impact of physical parameterization schemes on numerical simulation of super cyclone Gonu*, Natural Hazards. *55*, 211–231 DOI 10.1007/s11069-010-9521-x.

Deshpande, M.S., Pattnaik, S., and Salvekar, P.S. (2012), *Impact of cloud physical parameterization on the numerical simulation of a super cyclone*, Ann. Geophys. *30*, 775–795.

Dudhia, J. (1989), *Numerical study of convection observed during the winter monsoon experiment using a mesoscale two-dimensional model*, J. Atmos. Sci. *46*, 3077–3107.

Emanuel, K. (2005), *Increasing destructiveness of tropical cyclones over the past 30 years*, Nature, *436*, 636–638 doi: 10.1038/nature03906.

Govindankutty, M., Chandrasekar, A., and Pradhan, D. (2010), *Impact of 3DVAR assimilation of Doppler Weather Radar wind data and IMD observation for the prediction of a tropical cyclone*, Intern. Jour. Rem. Sensing. *31*(24) 6327–6345. http://dx.doi.org/10.1080/01431160903413689.

Hong, S.Y., Noh, Y., and Dudhia, J. (2006), *A new vertical diffusion package with an explicit treatment of entrainment processes*, Mon Weather Rev. *134*, 2318–2341.

IMD (2013), Very severe cyclonic storm, Phailin over the Bay of Bengal (08-14 October 2013): A Report, Cyclone Warning Division, India Meteorological Department, New Delhi.

Kotal, S.D., Bhattacharya, S.K., Roy Bhowmik, Rama Rao, Y.V., and Sharma, A. (2013), Report on very severe cyclonic storm Phailin over the Bay of Bengal, IMD (NWP Division) ESSO Ministry of Earth Sciences.

Kotal, S. D., and Roy Bhowmik, S. K. (2011), *A Multimodel Ensemble (MME) Technique for Cyclone Track Prediction over the North Indian Sea*, Geofizika. *28*(2), 275–291.

Kumar, A., Done, J., Dudhia, J., and Niyogi, D. (2011), *Simulations of cyclone Sidr in the Bay of Bengal with a high-resolution model: Sensitivity to large-scale boundary forcing*, Meteorol. Atmos. Phys. *114*, 123–137, DOI 10.1007/s00703-011-0161-9.

Kumar, R. A., Dudhia, J., and Roy Bhowmik, S. K. (2010), *Evaluation of physics options of the Weather Research and Forecasting (WRF) Model to simulate high impact heavy rainfall events over Indian Monsoon region*, Geofizika. *27*(2), 101–125.

Lin, Y.L., Farley, R.D., and Orville, H.D. (1983), *Bulk parameterization of the snow field in a cloud model*, J. Climate Appl Meteorol. *22*, 1065–1092.

Mandal, M., and Mohanty, U.C. (2006), *Impact of satellite derived wind in mesoscale simulation of Orissa super cyclone*, Indian Jou. Marine Sci. *35*(2) 161–173.

Mandal, M., Mohanty, U.C., and Raman, S. (2004), *A study on the parameterization of physical processes on prediction of tropical cyclones over the Bay of Bengal with NCAR/PSU mesoscale model*, Natural Hazards. *31*(2), 391–414.

Mandal, M., Mohany, U.C., Potty, K.V.J., and Sarkar, A. (2003), *Impact of horizontal resolution on prediction of tropical cyclones over Bay of Bengal using a regional weather prediction model*, Indian Acad. Sci. (Earth Planet. Sci.), *112*(1), 79–93.

Mishra, D.K., and Gupta, G.R. (1976), *Estimation of max wind speed in tropical cyclone occurring in India Seas*, Indian J. Met. Hydro. Geophys. *27*(3), 285–290.

Mlawer, E.J., Taubman, S.J., Brown, P.D., Iacono, M.J., and Clough, S.A. (1997), *Radiative transfer for inhomogeneous atmosphere: RRTM, a validated correlated-k model for the longwave*, J Geophys Res. *102*(D14), 16663–16682.

Mohanty, U.C., Osuri, K.K., Routray, A., Mohapatra, M., and Pattanayak, S. (2010), *Simulation of Bay of Bengal tropical cyclones with WRF model: Impact of initial and boundary conditions, Marine Geodesy*. *33*, 294–314. DOI: 10.1080/01490419.2010.518061.

Mohapatra, M., Nayak, D. P., Sharma, R. P., and Bandyopadhyay, B. K. (2013), *Evaluation of official tropical cyclone track forecast over north Indian Ocean issued by India Meteorological Department*, J. Earth Syst. Sci. *122*(3), 589–601.

Mohapatra, M., Bandyopadhyay, B. K., and Nayak, D. P. (2013), *Evaluation of operational tropical cyclone intensity forecasts over north Indian Ocean issued by India Meteorological Department*, Natural Hazards. *68*(2), 433–451, DOI 10.1007/s11069-013-0624-z.

Osuri, K.K., Mohanty, U.C., Routray, A., and Mohapatra, M. (2012), *The impact of satellite-derived wind data assimilation on track, intensity and structure of tropical cyclones over the North Indian Ocean*, Inter. Jour. Rem. Sensing. *33*(5) 1627–1652. http://dx.doi.org/10.1080/01431161.2011.596849.

Osuri, K.K., Mohanty, U.C., Routray, A., Makarand, A.K., and Mohapatra, M. (2011), *Customization of WRF-ARW model with physical parameterization schemes for the simulation of tropical cyclones over North Indian Ocean*, Natural Hazards. DOI 10.1007/s11069-011-9862-0.

Pan, H.L., and Wu, W.S. (1995), Implementing a mass flux convective parameterization package for the NMC medium-range forecast model. NMC Office Note 409, 40 pp. [Available from NCEP/EMC, 5200 Auth Rd., Camp Springs, MD 20746].

Pattanayak, S., Mohanty, U.C., and Osuri, K.K. (2012), *Impact of Parameterization of Physical Processes on Simulation of Track and Intensity of Tropical Cyclone Nargis (2008) with WRF-NMM Model*", The Scientific World Journal, Volume *2012*, Article ID 671437, 18 doi:10.1100/2012/671437.

Pattnayak, S., and Mohanty, U.C. (2008), *A comparative study on performance of MM5 and WRF models in simulation of tropical cyclones over Indian seas*", Curr. Sci. *95*, 923–936.

Pielke, R. A., Matsui, T., Leoncini, G., Nobis, T., Nair, U., Lu, E., Eastman, J., Kumar, S., Peters, C.L., Tian, Y., and Walko, R. (2006), *A new paradigm for parameterizations in numerical weather prediction and other atmospheric models*, National Wea. Digest. *30*, 93–99.

Raju, P.V.S., Potty, J., and Mohanty U.C. (2011), *Prediction of severe tropical cyclones over the Bay of Bengal during 2007–2010 using high-resolution mesoscale model*, Natural Hazards. DOI 10.1007/s11069-011-9918-1.

Rakesh, V., and Goswami, P. (2011), *Impact of background error statistics on forecasting of tropical cyclones over the north Indian Ocean*, Jour. Geophys. Research. *116*, DOI: 10.1029/2011JD015751.

Rakesh, V., Singh, R., and Joshi, P.C., (2009), *Intercomparison of the performance of MM5/WRF with and without satellite data assimilation in short-range forecast applications over the Indian region*, Meteorol Atmos. Phys. *105*, 133–155 DOI 10.1007/s00703-009-0038-3.

Routray, A., Mohanty, U.C., Rizvi, S.R.H., Niyogi, D., Osuri, K.K., and Pradhan, D. (2010), *Impact of doppler weather radar data on numerical forecast of Indian monsoon depressions*, Q.J.R. Meteorol. Soc. DOI:10.1002/qj.678.

Roy Bhowmik, S.K. (2003), *Prediction of monsoon rainfall with a nested grid mesoscale limited area model*, Proc Indian Acad. Sci. Earth Planet Sci. *112*, 499–519.

Sandeep, S., Chandrasekar, A., and Singh, D. (2006), *The impact of assimilation of AMSU data for the prediction of a tropical cyclone over India using a mesoscale model*, Intern. Jour. Remo. Sensing. *27*, 4621–4653.

Singh, R., Kishtwal, C.M., Pal, P.K., and Joshi, P.C. (2011), *Assimilation of the multisatellite data into the WRF model for track and intensity simulation of the Indian Ocean tropical cyclones*, Meteorol. Atmos. Phys. *111*, 103–119. DOI 10.1007/s00703-011-0127-y.

Singh, R., Pal, P.K., Kishtawal, C.M., and Joshi, P.C. (2008), *The impact of variational assimilation of SSM/I and QSCAT satellite observations on the numerical simulation of Indian Ocean Tropical Cyclones*, Wea Forecat. *23*, 460–476.

Singh, S.K., Kishtawal, C.M., and Pal, P.K. (2012), *Track prediction of Indian Ocean cyclones using Lagrangian advection model*. Natural Hazards. DOI 10.1007/s11069-012-0121-9.

Skamarock, W.C., Klemp, J.B., Dudhia, J., Gill, D.O., Barker, D.M., Wang, W., and Powers, J.G. (2008), A description of the advanced research WRF version 3, NCAR TECHNICAL NOTE.

Srinivas, C.V., Yesubabu, V., Hariprasad, R. B. R. R., and Ramarkrishna, S. S. V., Venkatraman B. (2013), *Real time prediction of a severe cyclone Jal over Bay of Bengal using a high-resolution mesoscale model WRF-ARW*, Natural Hazards. *65*, 331–357. DOI 10.1007/s11069-012-0364-5.

Srinivas, C.V., Bhaskar Rao, D.V., Yesubabu, Y., Baskaran, R., and Venkatraman, B. (2012), *Tropical cyclone predictions over the Bay of Bengal using the high-resolution Advanced Research Weather Research and Forecasting (ARW) model*, Q. J. R. Meteorol. Soc. DOI:10.1002/qj.2064.

Srinivas, C.V, Yesubabu V., Venkatesan, R., and Ramarkrishna, S.S.V.S. (2010), *Impact of assimilation of conventional and satellite meteorological observations on the numerical simulation of a Bay of Bengal Tropical Cyclone of November 2008 near Tamilnadu using WRF model*, Meteorol Atmos Phys. *110*, 19–44. DOI 10.1007/s00703-010-0102-z.

Srinivas, C.V., Venkateshan, R., Bhaskar Rao, D.V. and Prasad, D.H. (2007), *Numerical Simulation of Andhra Severe Cyclone (2003): Model Sensitivity to the Boundary Layer and Convection Parameterization*, Pure Appl. Geophys. *164*, 1465–1487.

Stoelinga, M.T. (1996), *A potential vorticity based study of the role of diabatic heating and friction in a numerically simulated baroclinic cyclone*, Mon. Wea. Rev. *124*, 849–874.

Tyagi A., Bandyopadhyay B. K., and Mohapatra, M. (2010), Monitoring and prediction of cyclonic disturbances over North Indian Ocean by Regional Specialised Meteorological Centre, New Delhi (India): Problems and prospective. In Indian Ocean Tropical Cyclones and Climate Change, Springer-Verlag, Berlin, 93–103.

Zhang, F., Weng, Y., Gamache, J. F., and Marks, F. D. (2011), *Performance of convection-permitting hurricane initialization and prediction during 2008–2010 with ensemble data assimilation of inner core airborne Doppler radar observations*, Geophys. Res. Lett. *38*, doi:10.1029/2011GL048469.

(Received June 9, 2014, revised April 6, 2015, accepted October 28, 2015, Published online November 23, 2015)